

Detecting and Locating Power Quality Issues by Implementing Wavelet Transform

Mohammad Asadi
Electricity Distribution
Company of Mazandaran
Sari, Iran

Mehrshad Noori Harikandeh
Electrical and Computer
Engineering Faculty
Islamic Azad University
Ghaemshahr, Iran

Mohammadreza Hamzenia
Electrical and Computer
Engineering Faculty
Islamic Azad University
Ghaemshahr, Iran

Abstract: Lack of power quality imposes many costs on large and small consumers every year. Therefore, considering the importance of power quality in today's industries, this article examines the issue of detection and location of various power quality issues. DWT discrete wavelet transform is investigated in this paper. The signals under the perturbations are written to the field and the start and end times of the perturbation are obtained and compared with the real time, and the accuracy of the measurements is confirmed by repetitions.

Keywords: flicker; power quality; voltage sag; voltage swell; wavelet transform

1. INTRODUCTION

The issue of power quality has been discussed since the beginning of the knowledge of electricity, but what was considered as electricity quality in the past, due to lack of sensitivity of consumers, their connection or disconnection. Today, the quality of electricity has become very important. This importance can be attributed to reasons such as the greater sensitivity of industrial loads, increased linear loads, increased use of small power plants and, most importantly, increased costs due to its absence [1-4]. Lack of power quality imposes a lot of costs on consumers, large and small, every year due to their load to voltage sensitivity. For example, many home appliances are damaged by these annual disturbances. As a result, identifying, monitoring, and controlling these disturbances with phasor measurement units (PMUs) can prevent significant damages [5]. Although the voltage stability, in the industry has been discussed for several years, there are still no standardized definitions in some areas. According to the IEEE1159 standard, power quality disturbances are classified into seven groups: transients [6], long-term voltage changes, short-term voltage changes [5], waveform distortions, voltage imbalances, flicker, and frequency changes, each of which in turn follows Branches are divided [7].

Voltage sags and voltage surges are classified in the group of short-term voltage and harmonic changes in the group of waveform distortions [8]. These perturbations have been studied in this work. Various tools have been used to analyze power quality perturbations. One of the tools that is becoming more and more popular is the Wavelet Converter [9]. Wavelet converter is a mathematical tool that scans data, functions, or operators into different frequency components and then studies each component with resolution according to its scale. For example, in signal analysis, wavelet transform allows us to view the time history in terms of the frequency components of the signal [10]. This article provides an overview of wavelet transform and applications of wavelet transform in power systems.

2. WAVELET TRANSFORM AS A DETECTION AND LOCATION TOOL

Most current methods for detecting power quality perturbations have their limitations and are implemented directly in the time field. In this paper, a proposal for detection and localization of perturbations based on orthogonal wavelet transform is presented in which time-scale field detection is performed [11]. As will be shown in the next section, this proposition is useful in detecting a wide range of power quality perturbations such as rapid voltage fluctuations, short-term voltage changes, and harmonic perturbations [12].

The detection method is almost straightforward. The given waveform is transmitted to the time-scale field using Multiple Signal Detection (MSD) analysis. Normally, single or double scale signal analysis is appropriate to distinguish perturbations from their backgrounds, because the decomposed signals at lower scales (higher frequencies) have high temporal location. In other words, high-scale signal analysis is not necessary because it gives poor temporal positioning. Suppose we have a special type of mother wavelet with L filter coefficient, $h(n)$ and $g(n)$, which form a family of wavelet functions $\phi(t)$ and scale functions $\psi(t)$, respectively [13].

$$\varphi(t) = \sqrt{2} \sum_n h(n) \Phi(2t - n) \quad (1)$$

$$\Psi(t) = \sqrt{2} \sum_n g(n) \Psi(2t - n) \quad (2)$$

As a result, the process of detection and localization is a set of processes of convolution and dissimulation at the corresponding scale. In scale one, the electrical power signal $c_0(n)$ with N sampling point is decomposed into two other signals. $c_1(n)$ and $d_1(n)$ are defined as follows:

$$c_1(n) = \sum_k h(k - 2n) c_0(k) \quad (3)$$

$$d_1(n) = \sum_k g(k - 2n) c_0(k) \quad (4)$$

The signal $c_1(n)$ is the smoothed model of the original signal $c_0(n)$ while the model $d_1(n)$ is the detail of the main signal which is in the form of wavelet transform coefficients (WTCs) on a scale of one. These coefficients provide detection information. In cases of power quality perturbations, whenever perturbations occur in a given sine waveform, WTCs are exclusively larger than their adjacent coefficients [14]. Transform of wavelets to signals with sensitive disturbances. But its behavior is "blind" to fixed behavior signals (i.e., a 60 Hz sine waveform) [15]. By considering this process, one can assume that the physical understanding of detection and location described in (3) and (4) is as follows:

$$c_1(n) = \int f(t) \varphi_{1,n}(t) dt = \frac{1}{\sqrt{2}} \int f(t) \varphi\left(\frac{t}{2} - n\right) dt \quad (5)$$

$$d_1(n) = \int f(t) \psi_{1,n}(t) dt = \frac{1}{\sqrt{2}} \int f(t) \psi\left(\frac{t}{2} - n\right) dt \quad (6)$$

where:

$$f(t) = \sum_n c_0(n) \varphi(t-n) = \sum_n c_0(n) \varphi_{0,n}(t) \quad (7)$$

In (7) it can be considered as a "dummy signal" generated by a linear combination with a scale function at zero scale. So, any disturbance in will be well manifested. By placing (1) and (2) in (5) and (6) we will have:

$$c_1(n) = \int f(t) \sum_k h(k) \varphi(t-2n-k) dt \quad (8)$$

$$d_1(n) = \int f(t) \sum_k g(k) \varphi(t-2n-k) dt \quad (9)$$

It can be inferred from Equation (8) that $c_1(n)$ is the smoothed model of the main signal $c_0(n)$, because $h(n)$ has a low-frequency response. Whereas from (9) it is obvious that contains only frequency components higher than the signal $f(t)$ because $g(n)$ has a high-pass filter response. This explains why the analysis of wavelet transform is sensitive to signals with large perturbations but is "blind" to perturbations of constant behavior. In practice, it is not necessary to construct $f(t)$, but it is useful in understanding the physical process of detection and location as expressed in (5) and (6). In fact, the signals are obtained directly from Equations (3) and (4). This greatly simplifies the detection and location process [16]. The detection process for the second scale $c_1(n)$ starts from the signal in which this signal can be considered as a new $c_0(n)$. The above process is repeated. Because wavelet and scale functions become wider as the scale increases, temporal location is lost. It is suggested that higher scale decomposition is not necessary. As long as the detection of disturbances in power systems is desired, two-scale signal analysis of the original signal is sufficient to detect and locate the disturbances [17].

3. SIMULATION AND RESULTS

3.1 Data Production

Table 1 can be used to generate power quality phenomena and its parameters can be controlled. This work focuses on the phenomena of voltage dip, voltage swell, harmonic, harmonic and flicker. The length and amplitude of perturbations are defined by IEEE1159.

The voltage flicker can be seen as a carrier wave that changes the amplitude modulation at a frequency of 30Hz~1kHz. The flicker signal $u(t)$ is expressed as follows:

$$u(t) = V_m [1 + m \cos(\Omega t)] \cos(\omega_0 t) \quad (10)$$

where, V_m is voltage amplitude at power frequency, ω_0 is the angular frequency of the carrier wave, m is the amplitude of the carrier wave voltage (modulation parameter), $m \cos(\Omega t)$ is the flicker voltage and Ω is the angular frequency of the amplitude modulation voltage. A flicker signal is generated to simulate with following parameters:

$$u(t) = V_m [1 + m a(t)] \cos(\omega_0 t) \quad (11)$$

That

$$\omega_0 = 100\pi \frac{\text{rad}}{\text{s}}, V_m = 0.1V$$

$$a(t) = \cos(\Omega t) + \frac{1}{3} \cos(3\Omega t) + \frac{1}{5} \cos(5\Omega t) \quad (12)$$

When there is Flicker, $m=1$ and otherwise $m=0$. The desired signals are generated and simulated in Matlab environment and then analyzed in Wavelet field. All times presented in the rest of the article are generated randomly. All times are in seconds.

3.2 Voltage Sag and Protrusion

The main wavelet function db4 was used for analysis. It can be seen that the details of the first level are sufficient to detect the phenomena. For example, look at the voltage drop phenomenon in Figure 1. Figure 1(a) shows the perturbation signal and Figure 1(b) shows the details of the first level.

As we can see, the start and end times of the disturbance became very clear. For this particular example, the occurrence and termination times are 0.0248 and 0.0349, respectively, and the program detects the times 0.0250 and 0.0352, which is a good approximation. The actual error length is 0.0101 and the calculated length is 0.0102, which indicates an error of 1% in calculating the error length.

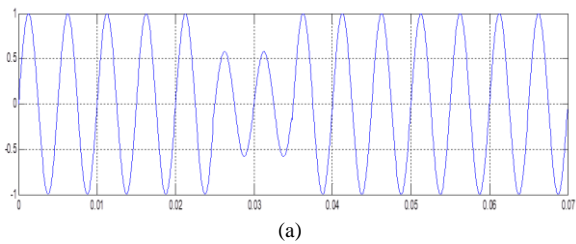
Figure 2 shows a voltage swell. As we can see from Table 2, the actual and obtained times for the onset, end, and length of the perturbation are significantly closer.

So far, we have uncovered these two phenomena. If the standard deviation curve of the details is drawn at different levels, a distinction can be made between these two perturbations. Figure 3 shows the standard deviation curve of the high voltage sag and protrusion and a pure sine wave. We see that the maximum standard deviation of the coefficients in the voltage rise is greater than this value in the pure sine wave, while the maximum standard deviation of the coefficients in the voltage sag is less than its corresponding value in the pure sine wave. The parameters of this perturbation and the actual and obtained times are given in Table 2.

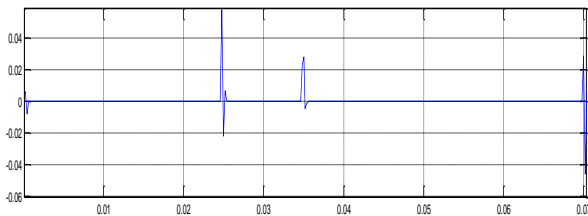
The accuracy of the results expressed in the program repetitions is also repeated.

Table 1. Model of power quality perturbation

Power quality perturbation	Model	Parameters
Sinusoidal	$x(t) = \sin(\omega t)$	
Voltage Swell	$x(t) = A(1 + \alpha(u(t - t_1) - u(t - t_2)))\sin(\omega t)$ $t_1 < t_2, u(t) = \begin{cases} 1, & t \geq 0 \\ 0, & t < 0 \end{cases}$	$0.1 \leq \alpha \leq 0.8$ $T \leq t_2 - t_1 \leq 9T$
Voltage Sag	$x(t) = A(1 - \alpha(u(t - t_1) - u(t - t_2)))\sin(\omega t)$	$0.1 \leq \alpha \leq 0.9$ $T \leq t_2 - t_1 \leq 9T$
Harmonic	$x(t) = A(\alpha_1 \sin(\omega t) + \alpha_3 \sin(3\omega t) + \alpha_5 \sin(5\omega t) + \alpha_7 \sin(7\omega t))$	$0.05 \leq \alpha_3 \leq 0.15, 0.05 \leq \alpha_5 \leq 0.15,$ $0.05 \leq \alpha_7 \leq 0.15, \sum \alpha_i^2 = 1$
Voltage swell with Harmonic	$x(t) = A(1 - \alpha(u(t - t_1) - u(t - t_2)))$ $(\alpha_1 \sin(\omega t) + \alpha_3 \sin(3\omega t) + \alpha_5 \sin(5\omega t))$	$0.1 \leq \alpha \leq 0.9, T \leq t_2 - t_1 \leq 9T$ $0.05 \leq \alpha_3 \leq 0.15, 0.05 \leq \alpha_5 \leq 0.15,$ $\sum \alpha_i^2 = 1$
Voltage Sag with Harmonic	$x(t) = A(1 + \alpha(u(t - t_1) - u(t - t_2)))$ $(\alpha_1 \sin(\omega t) + \alpha_3 \sin(3\omega t) + \alpha_5 \sin(5\omega t))$	$0.1 \leq \alpha \leq 0.9, T \leq t_2 - t_1 \leq 9T$ $0.05 \leq \alpha_3 \leq 0.15, 0.05 \leq \alpha_5 \leq 0.15,$ $\sum \alpha_i^2 = 1$

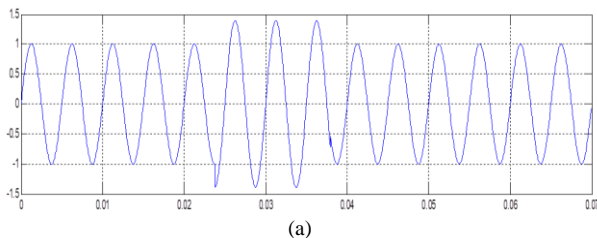


(a)

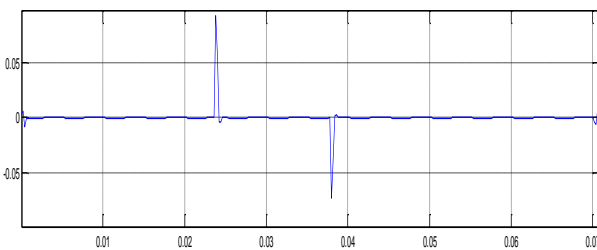


(b)

Figure 1. (a) An example of a voltage sag, (b) Details of the first level



(a)



(b)

Figure 2. (a) A voltage swell, (b) The first level details

Table 2. The parameters of the voltage swell

Calculated Start Time	Calculated End Time	Calculated Length	Error %
0.0240	0.0382	0.0142	0.5351
Real Time Start	Real Time End	Voltage Sag Range	Actual Length
0.0238	0.0380	1.3934	0.0141

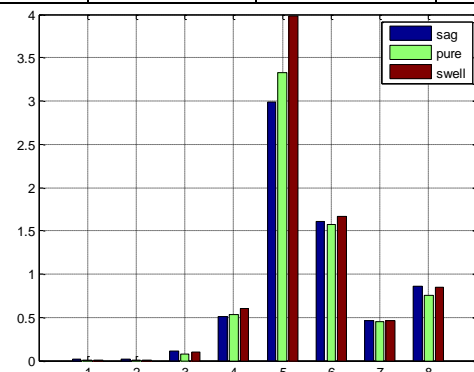


Figure 3. Standard deviation curve at different levels

3.3 Voltage Sag with Harmonic, Voltage Rise with Harmonic

Again, the db4 function is used in this section. Figure 4 shows a voltage sag in the presence of a harmonic perturbation.

Figure 5 shows a harmonic voltage rise. Actual and calculated start and end times as well as actual and calculated error lengths are given in Table 3. A small error of 0.8547% also confirms the correctness of the proposed algorithm. The accuracy shown demonstrates the advantage of wavelet transform in investigating this perturbation.

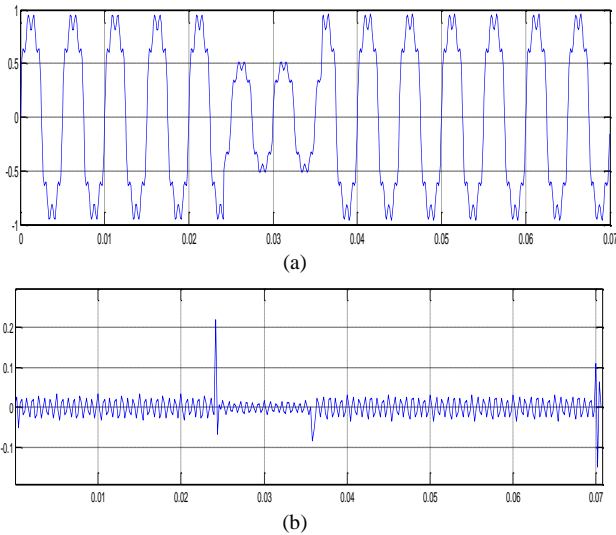


Figure 4. (a) A recess with a harmonic, (b) The first level details

Table 3. The parameters of the harmonica sag phenomenon

Calculated Start Time	Calculated End Time	Calculated Length	Error %
0.0244	0.0360	0.0116	0.8547
Real Time Start	Real Time End	Voltage Sag Range	Actual Length
0.0243	0.0359	0.5398	0.0117
$h_3=0.1417$	$h_5=0.0786$	$h_7=0.1257$	

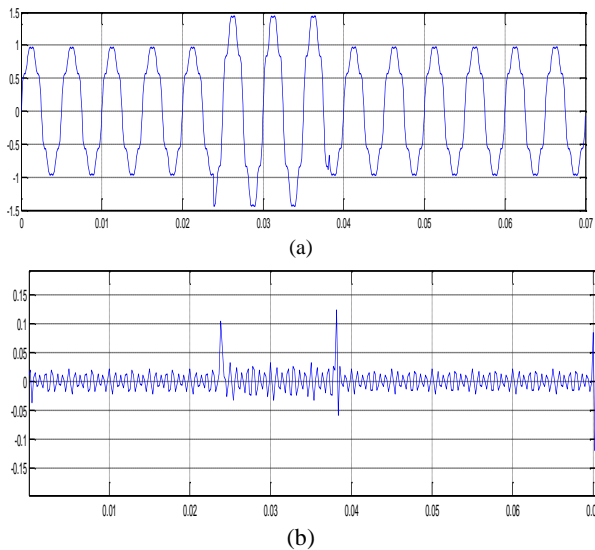


Figure 5. (a) Voltage swell with Harmonic (b) The first level details

The harmonic addition does not change what was said about the standard deviation of the detail coefficients in the previous section, and it still works to distinguish between indentations and ridges. That is, the maximum standard deviation of the details at different levels in the voltage sag is less than the pure sine wave, while this value will be greater in the voltage swell than the sine wave.

3.4 Flicker

Suppose there is a voltage flicker sample similar to following equation.

$$u(t) = V_m [1 + m a(t)] \cos(\omega_0 t) \quad (13)$$

That

$$\omega_0 = 100\pi \frac{\text{rad}}{\text{s}}, V_m = 0.1V$$

$$a(t) = \cos(\Omega t) + \frac{1}{3} \cos(3\Omega t) + \frac{1}{5} \cos(5\Omega t) \quad (14)$$

The signal is simulated and written to the wavelet. By comparing different wavelets in Matlab, db24 was selected as a suitable wavelet. By observing the details and approximations at different levels, it can be seen that the details of the first level have the ability to detect the start and end times of this phenomenon (Figure 6). The various parameters of this perturbation are given in Table 4. A negligible error of 0.29% indicates the efficiency of this algorithm in voltage flicker detection.

Table 4. Parameters of the phenomenon of voltage swell with harmonic

Calculated Start Time	Calculated End Time	Calculated Length	Error %
0.0384	0.0240	0.0144	0.7100
Real Time Start	Real Time End	Voltage Sag Range	Actual Length
390.02	0.0382	1.4869	0.0143
$h_3=0.0584$	$h_5=0.0900$	$h_7=0.0760$	

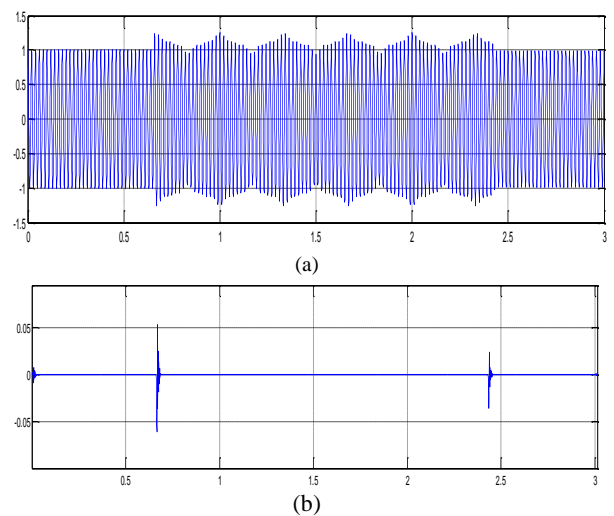


Figure 6. (a) An example of a voltage flicker, (b) Details in the first level

4. CONCLUSION

This article presents a suggestion for detecting and locating power quality phenomena. The perturbations of voltage dip, voltage swell, harmonic dip, harmonic swell and flicker are simulated and plotted in the Wavelet field. The ability of this transform to decompose waveforms into different levels of detail and approximation made it possible to detect these phenomena. The start and end times and the length of the error are obtained with good accuracy. Also, with the help of standard deviation of detail coefficients at different levels, a distinction is made between the two phenomena of sag and voltage swell.

5. REFERENCE

- [1] O. P. Mahela, B. Khan, H. H. Alhelou, and S. Tanwar, "Assessment of power quality in the utility grid integrated with wind energy generation," *IET Power Electronics*, vol. 13, pp. 2917-2925, 2020.
- [2] O. P. Mahela, B. Khan, H. H. Alhelou, and P. Siano, "Power quality assessment and event detection in distribution network with wind energy penetration using stockwell transform and fuzzy clustering," *IEEE Transactions on Industrial Informatics*, vol. 16, pp. 6922-6932, 2020.
- [3] H. Shokouhandeh, M. Ghaharpour, H. G. Lamouki, Y. R. Pashakolaie, F. Rahmani, and M. H. Imani, "Optimal Estimation of Capacity and Location of Wind, Solar and Fuel Cell Sources in Distribution Systems Considering Load Changes by Lightning Search Algorithm," in *2020 IEEE Texas Power and Energy Conference (TPEC)*, 2020, pp. 1-6.
- [4] C. Diaz, F. Ruiz, and D. Patino, "Analysis of water booster pressure systems as dispatchable loads in smart-grids," in *2017 IEEE PES Innovative Smart Grid Technologies Conference Europe (ISGT-Europe)*, 2017, pp. 1-6.
- [5] H. Haggi, W. Sun, and J. Qi, "Multi-Objective PMU Allocation for Resilient Power System Monitoring," in *2020 IEEE Power & Energy Society General Meeting (PESGM)*, 2020, pp. 1-5.
- [6] S. Khazaei, M. Hayerikhiyavi, S. M. Kouhsari, "A Direct-Based Method for Real-Time Transient Stability Assessment of Power Systems", *CRPASE* Vol. 06(02), 108-113, June 2020.
- [7] M. Bajaj and A. K. Singh, "Grid integrated renewable DG systems: a review of power quality challenges and state-of-the-art mitigation techniques," *International Journal of Energy Research*, vol. 44, pp. 26-69, 2020.
- [8] H. Shokouhandeh and M. Jazaeri, "An enhanced and auto-tuned power system stabilizer based on optimized interval type-2 fuzzy PID scheme," *International Transactions on Electrical Energy Systems*, vol. 28, p. e2469, 2018.
- [9] W. Qiao and Z. Yang, "Forecast the electricity price of US using a wavelet transform-based hybrid model," *Energy*, vol. 193, p. 116704, 2020.
- [10] S. Kumar, R. Kumar, R. P. Agarwal, and B. Samet, "A study of fractional Lotka-Volterra population model using Haar wavelet and Adams-Bashforth-Moulton methods," *Mathematical Methods in the Applied Sciences*, vol. 43, pp. 5564-5578, 2020.
- [11] S. K. Khare, V. Bajaj, and G. Sinha, "Adaptive Tunable Q Wavelet Transform-Based Emotion Identification," *IEEE transactions on instrumentation and measurement*, vol. 69, pp. 9609-9617, 2020.
- [12] M. Asadi, H. Shokouhandeh, F. Rahmani, S. M. Hamzehnia, M. N. Harikandeh, H. G. Lamouki, *et al.*, "Optimal placement and sizing of capacitor banks in harmonic polluted distribution network," in *2021 IEEE Texas Power and Energy Conference (TPEC)*, 2021, pp. 1-6.
- [13] F. Z. Dekhandji, "Detection of power quality disturbances using discrete wavelet transform," in *2017 5th International Conference on Electrical Engineering-Boumerdes (ICEE-B)*, 2017, pp. 1-5.
- [14] R. Kumar and H. O. Bansal, "Hardware in the loop implementation of wavelet based strategy in shunt active power filter to mitigate power quality issues," *Electric Power Systems Research*, vol. 169, pp. 92-104, 2019.
- [15] H. Shokouhandeh, M. Jazaeri, and M. Sedighzadeh, "On-time stabilization of single-machine power system connected to infinite bus by using optimized fuzzy-PID controller," in *2014 22nd Iranian Conference on Electrical Engineering (ICEE)*, 2014, pp. 768-773.
- [16] B. Eristi, O. Yildirim, H. Eristi, and Y. Demir, "A new embedded power quality event classification system based on the wavelet transform," *International Transactions on Electrical Energy Systems*, vol. 28, p. e2597, 2018.
- [17] H. Huang, R. He, Z. Sun, and T. Tan, "Wavelet-srnet: A wavelet-based cnn for multi-scale face super resolution," in *Proceedings of the IEEE International Conference on Computer Vision*, 2017, pp. 1689-1697.

Performance of Solar Energy Watering Cassava Crop Systems with Systems Control by Smartphone

Thep Kueathaweekun
Faculty of Industrial
Technology
Kamphaeng Phet Rajabhat
University
Kamphaeng Phet Rajabhat,
Thailand

Pakin Maneechot
Faculty of Industrial
Technology
Kamphaeng Phet Rajabhat
University
Kamphaeng Phet Rajabhat,
Thailand

Jaturong Thongchai
Faculty of Industrial
Technology
Kamphaeng Phet Rajabhat
University
Kamphaeng Phet Rajabhat,
Thailand

Jarukit Piboolnaruedom
Faculty of Industrial
Technology
Kamphaeng Phet Rajabhat
University
Kamphaeng Phet Rajabhat,
Thailand

Abstract: In this paper, design and development solar energy watering cassava crop systems with systems control by smartphone is presented. The objective is study the performance of the watering system by smartphones. The hardware component was Arduino Uno, Wi-Fi module, water pump, relay, solar panels, battery, smart phone and blynk applications, respectively. The design and development of the prototype watering cassava crop system with controlled by smartphones and write program command code for systems control by using blynk applications. This research was studied working distance incase with or without obstruction and studied working of water pump and solenoid valve, respectively. From the experiment results of the solar energy watering cassava crop systems that smartphone can ON-OFF solenoid valve to open or close water flow of 0-50 meters (diameter =100 m) in case without obstruction, 0-30 meters (diameter = 60 m) in case with obstruction, working distance of moisture sensor of 0-90 meters, water pump and solenoid valve can work precisely, respectively. Moreover, the experimental results of monitoring of watering cassava crop system by smartphone as follows: the average temperature of 36C°, average ambient humidity of 50%, and average soil moisture of 60%, respectively. Therefore, the watering cassava crop systems with systems control using smartphone can use for the communities to reduce time, increase efficiency and increase the productivity of the community sustainably.

Keywords: Microcontroller; arduino; cassava; watering systems; solar cell

1. INTRODUCTION

Nowadays, water is very important for the cassava crop plant in Thailand. The volume cropping of cassava in 2020 in Thailand of 1.95 million acres. Various factors contribute to the yield of cassava crops such as proper soil preparation, different varieties of crops and respective techniques for production. The chemical fertilizer is volume added to the soil, various natural hazards occurring in the cultivated place, number of seeds added in the related area, proportion of moisture in the fields, plant disease detection and adoption of modern technologies, respectively. The water is a mainly factor to helping in the growth of cassava crop plant. In the summer season, the cassava crop plant need water for help watering of the plant. Since water in Thailand have the water limited. Therefore, if have the watering systems for management of the water. Currently, technology internet of thing (IoT) is technology for support management of the water. The mainly benefits that farmers get from IoT application in agriculture such as, increase in the yielding,

benefit is the cost of production, reduces the wastage coming from the production and automates the most of the processes, respectively.

Therefore, several researchers are design and development systems for agriculture plant. In 2013, the researcher designed a system that can be controlled its performances using short text message (SMS) from the cell phone [1-3]. This research has been implemented the monitoring systems by using GSM with a digital mobile telephone system. According to Louis D. Albright, Robert W. Langhans (2015), the author used sensor devices coupled with wireless technologies to monitor the temperature, humidity and moisture [4]. The details of their ideas are having a wireless sensor that connects through a Wi-Fi to a Central Monitoring Station through General Packet Radio Station. In addition, it also connects with Global Positioning System (GPS) to send message to the central monitoring station. The other researcher is studied online control of remote agricultural robots operated using fuzzy controllers and virtual instrumentation. The system in the robot consisted of a microcontroller, a DC motor, and a Fuzzy

logic controller algorithm [5]. Polpitiya and et. al. are design wireless agricultural sensor networks consisting of a temperature sensor, a humidity sensor, a pH level sensor, a light sensor, a microcontroller, and a WSN [6]. The monitored and controlled the aeroponic growth system for potato production by Idris and Muhammad Ikhsan Sani. This system consisted of a microcontroller, a temperature sensor and pH, humidity, and fogging sensors [7]. Mahamai, P. et al. [8] have proposed automatic watering using solar PV tracking to the longan. This application is suitable for areas without electricity system. The research in [9] proposed an automatic watering system by wireless network based on Arduino Uno R3 microcontroller and Xbee wireless module. In addition, the satisfaction of wireless communication is also considered. Some researchers have proposed microcontrollers based irrigation systems for solving a serious problem of food in India [10]-[11]. Nevertheless, we consider that those of the systems may also improve and deployment the growing up of vegetables and provide more agricultural outputs. A watering system should be modifying for increase performance and more control by using smartphone and use solar energy for support systems in the area without electricity. Therefore, it should be improving system for support solar energy watering cassava crop systems with systems control by smartphone.

In this paper presents design and development of watering cassava crop systems with systems control through smartphone by using solar energy. The objective is study the performance of the watering system by smartphones. The prototype of watering systems use hardware component are Arduino Uno, Wi-Fi module, water pump, relay, solar panels, battery, smart phone and blynk applications, respectively. This research is studied working distance incase with or without obstruction and studied working of water pump and solenoid valve, respectively. Improve the watering cassava crop systems with systems control using smartphone can use for the communities to reduce time, increase efficiency and increase the productivity of the community sustainably. Detail the experiment results and discussion show in next section.

2. THE MATERIAL AND METHODS

2.1 Hardware component

All this system some hardware components use for sensing the inputs signal and operate accurately to get the exact outputs. Arduino Uno are control the components by programming the software code.

2.1.1 Arduino Uno

Arduino Uno is Arduino boards used interfaced between various expansion boards and other circuits used for digital electronics. The Arduino UNO has 14 digital in/out pins and 6 Analog in/out pins. This analog in/out pins are best useful for analog sensor. In this system Arduino UNO board use as the brain that read input signal from the sensors and then process and generate output signal to the motor driver relay. Perform the necessary functions by connected the various components.

2.1.2 Soil Moisture Sensor

Soil Moisture Sensor has two conducting plates to sense the moisture level in the soil. The sensor measures the moisture level of the soil by passing electric current through the two plates. The soil conducts more electricity, lower resistance when there is more water. The soil conducts less electricity, higher resistance when there is dry, less water. The moisture sensor placed in the soil to measure the moisture level of soil.

2.1.3 Relay

Relay is devices that used low power signal to control another high power circuit while they are completely separate. It is electromagnetic device, which is use to connect two circuits magnetically and isolate them electrically. A relay switch can be divide into input and output. The input section has a coil, which generates magnetic field when a small voltage from an electronic circuit is apply to it. This voltage is call the operating voltage. Commonly used relays are available in different configuration of operating voltages. This research uses the relay modules that are powered using 3.3V, which is ESP8266.

2.1.4 Water power pump

Water power pump is a device that transfer water, fluids or liquids from lower place to higher place or far place by mechanical action. It can classify into three major groups according to the method they use to move the fluid direct lift, displacement, and gravity pumps. Pumps operate by some mechanism and it consume energy to perform mechanical work by moving the fluid. Pumps operate by many energy including manual operation electricity, engines, or wind power come in many sizes, from microscopic for use in medical applications to large industrial pumps. This research uses solar powered water pump DC 12V.

2.1.5 Solar cell

Solar cell is an electrical device that converts the energy of light directly into electricity by the photovoltaic effect, which is a physical and chemical phenomenon. It is a photoelectric cell defined as a device whose electrical characteristics, such as, current, voltage, or resistance, vary when exposed to light. Individual solar cell devices are often the electrical building blocks of photovoltaic modules, known colloquially as solar panels. This research uses solar panels of DC 12V, 150 W.

2.1.6 Battery

Battery is an advanced battery technology that uses lithium ions as a key component of its electrochemistry. During a discharge cycle, lithium atoms in the anode are ionized and separated from their electrons. This research use battery of DC 12V, 20 Ah.

2.1.7 Solenoid valve

Solenoid valve is a valve system by using electrical energy to control the valve opening and closing. By sending electrical energy to the magnetic coil and control valve for ON-OFF water systems.

2.1.8 Smartphone

Smartphone is a mobile or cellular phone that runs off a mobile operating system and functions like a mini computer. Smartphones also function as portable media players, digital cameras, video cameras and GPS navigational devices. The operating system equips the device with advanced computing capabilities, runs applications and enables the device to perform the following basic features.

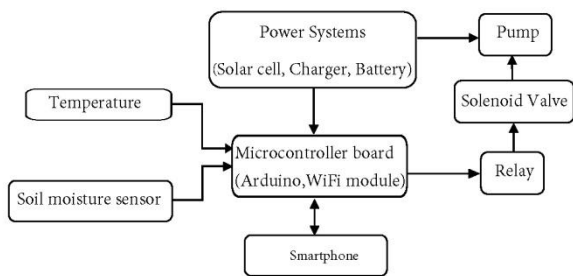
2.1.9 Blynk

Blynk is a platform with iOS and Android apps to control, ESP8266, Raspberry Pi and the likes over the Internet. It has can easily build graphic interfaces for all your projects by simply dragging and dropping widgets.

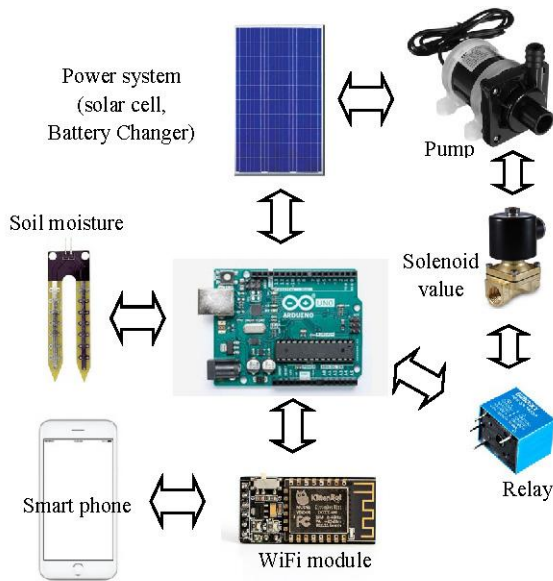
3. DESIGN of WATERING CASSAVA CROP SYSTEMS THROUGH SMART PHONE

3.1 Structure of watering cassava crop systems through smart phone

The design and development of solar energy watering cassava crop systems with systems control by smartphone. The structure of the proposed systems composes the prototype of a watering system and programming to control the operation of the watering system for cassava that is controlled by mobile phone. The block diagram of watering cassava crop systems through smart phone as shown in figure 1(a) and picture of watering cassava crop systems through smart phone, as shown in finger 1(b).



(a) Block diagram of watering cassava crop systems through smart phone



(b) Picture of watering cassava crop systems through smart phone

Figure 1. Watering Cassava Crop systems through Smart Phone

The design and development of watering cassava crop systems by control through smartphone as following:

1. Create the systems by connecting between device are the solar panel, the controller charger, battery, Arduino UNO control board, relay, water power pump to soil moisture sensor for control solenoid value ON-OFF system.

2. Microcontroller [12] board that is compatible with Arduino Uno and has ESP8266EX as an integrated Wi-Fi module. In this prototype for controls other electronic components such as soil moisture sensor, relay, solenoid valve and watering pipe. The ESP8266EX as the Wi-Fi module built-in the board, serve to connect the watering device.

3. Soil Moisture sensor [13] is to detect soil moisture or can be used to determine whether Moisture in the soil around the sensor. The soil moisture sensor is the sensor used to the soil to detect moisture.

4. When soil moisture has reached the specified value, it sends a command to the relay. The relay is device will act connected to the solenoid valve to open or close water flow.

5. Smartphone is device for control ON-OFF the water flow by Wi-Fi module with design command code for systems control by Blynk Apps [14].

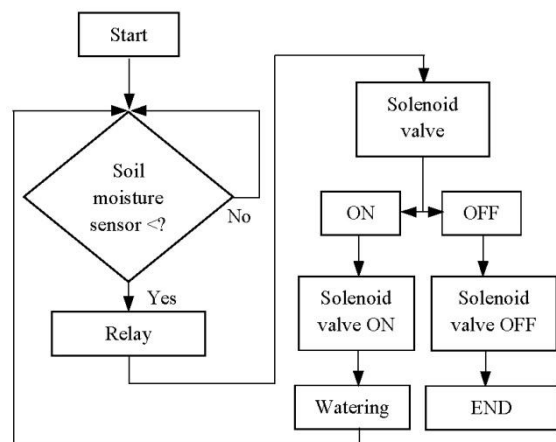
The prototype of watering cassava crop systems through smart Phone, as shown in figure 2.



Figure 2. Prototype of watering cassava crop systems through smart Phone

3.2 Controllable of the watering cassava crop systems through smartphone

The watering cassava crop systems through smartphone is presented. One part of systems is program command code for systems control by using Blynk apps installed on smartphone to control ON-OFF the watering systems, as show in figure 3.



(a) Block diagram



(b) Smartphone display

Figure 3. Smartphone display and block diagram of watering cassava crop systems through smart phone

From figure 3, show the smartphone display and block diagram of watering cassava crop systems through smart phone. This systems using Arduino Uno R3 will process to enter the process of sending on-off data to relay to turn ON-OFF electromagnetic valve through smartphone.

4. RESULTS OF WATERING CASSAVA CROP SYSTEMS

This researcher, we studied performance of solar energy watering cassava crop systems with systems control by smartphone as following:

4.1 The experiment working distance between cassava crop watering system and smartphone

First, the experiment working distance of watering systems for find distance between cassava watering system and smartphone in case without obstruction. In this case, we studied the performance of watering systems 5 trials and study distance of 10-100 meters. The experiment results are shown in table 1.

Table 1. Experiment results of distance between cassava crop watering system and smartphone in case without obstruction

Order	Experiment	Distance (m)									
		10	20	30	40	50	60	70	80	90	100
1	Working distance between cassava crop watering system and smartphone No. 1	✓	✓	✓	✓	✓	×	×	×	×	×
2	Working distance between cassava crop watering system and smartphone No. 2	✓	✓	✓	✓	✓	×	×	×	×	×

3	Working distance between cassava crop watering system and smartphone No. 3	✓	✓	✓	✓	✓	×	×	×	×	×
4	Working distance between cassava crop watering system and smartphone No. 4	✓	✓	✓	✓	✓	×	×	×	×	×
5	Working distance between cassava crop watering system and smartphone No. 5	✓	✓	✓	✓	✓	×	×	×	×	×

From the experiment results of the performance working watering systems for find distance between cassava crop watering system and smartphone in case without obstruction in table 1. The experiment results of systems can ON-OFF solenoid valve to open or close water flow from smartphone of 10-50 meters (diameter =100 m).

Second, the experiment working of watering systems for find distance between cassava watering system and smartphone in case with obstruction. In this case, we studied the performance of watering systems 5 trials and study distance of 10-100 meters. The experiment results as shown in table 2.

Table 2. Experiment results of distance between cassava crop watering system and smartphone in case with obstruction

Order	Experiment	Distance (m)									
		10	20	30	40	50	60	70	80	90	100
1	Working distance between cassava crop watering system and smartphone No. 1	✓	✓	✓	×	×	×	×	×	×	×
2	Working distance between cassava crop watering system and smartphone No. 2	✓	✓	✓	×	×	×	×	×	×	×
3	Working distance between cassava crop watering system and smartphone No. 3	✓	✓	✓	×	×	×	×	×	×	×
4	Working distance between cassava crop watering system and smartphone No. 4	✓	✓	✓	×	×	×	×	×	×	×
5	Working distance between cassava crop watering system and smartphone No. 5	✓	✓	✓	×	×	×	×	×	×	×

From the experiment results of the performance working watering systems for find distance between cassava crop watering system and smartphone in case with obstruction in

table 2. The experiment results of systems can ON-OFF solenoid valve to open or close water flow from smartphone of 0-30 meters (diameter = 60 m). The experiment, it was found that working distance decrease because obstruction.

4.2 The experiment working distance of moisture sensor

This section shows the experiment working distance of moisture sensor for open or close water flow. In this case, we studied the performance of watering systems in five trials and study distance of 10-100 meters. The experiment results are shown in table 3.

Table 3. The experiment working distance of moisture sensor

Order	Experiment	Distance (m)									
		10	20	30	40	50	60	70	80	90	100
1	working distance of moisture sensor No. 1	✓	✓	✓	✓	✓	✓	✓	✓	✓	✗
2	working distance of moisture sensor No. 2	✓	✓	✓	✓	✓	✓	✓	✓	✓	✗
3	working distance of moisture sensor No. 3	✓	✓	✓	✓	✓	✓	✓	✓	✓	✗
4	working distance of moisture sensor No. 4	✓	✓	✓	✓	✓	✓	✓	✓	✓	✗
5	working distance of moisture sensor No. 5	✓	✓	✓	✓	✓	✓	✓	✓	✓	✗

From table 3 show the experiment working distance of moisture sensor. The experiment results working distance of moisture sensor of 0-90 meters.

4.3 The experiment working of water pump and solenoid valve

This section shows the experiment working of water pump and solenoid valve in different conditions. In this case, we studied the performance of watering systems in five trials and study operation of the water pump and solenoid valve in different conditions. The experiment results as shown in table 4-5.

Table 4. Operation of the water pump in different conditions

Experiment	Pump status	
	close	open
Experiment No.1 (wet)	✓	-
Experiment No.2 (dry)	-	✓
Experiment No.3 (wet)	✓	-
Experiment No.4 (dry)	-	✓
Experiment No.5 (wet)	✓	-

From table 4 show the experiment of the operating water pump in different conditions. The experiment results of the operating water pump in case of wet, water pump of close (OFF) and in case dry, the water pump of open (ON), respectively.

Table 5. Operation of the solenoid valve in different conditions.

Experiment	Solenoid valve status	
	close	open
Experiment No.1 (wet)	✓	-
Experiment No.2 (dry)	-	✓
Experiment No.3 (wet)	✓	-
Experiment No.4 (dry)	-	✓
Experiment No.5 (wet)	✓	-

From table 5 show the experiment operating of the solenoid valve in different conditions. The experiment results of the operating solenoid valve in case of wet, solenoid valve of close (OFF) and in case dry, the solenoid valve of open (ON), respectively.

This section, we studied performance of solar energy watering cassava crop systems with systems control using smartphone in Kamphaeng Phet, Thailand. The monitoring of watering cassava crop systems consist temperature, moisture sensor and humidity sensor, respectively. The experiment results as shown in figure 4.

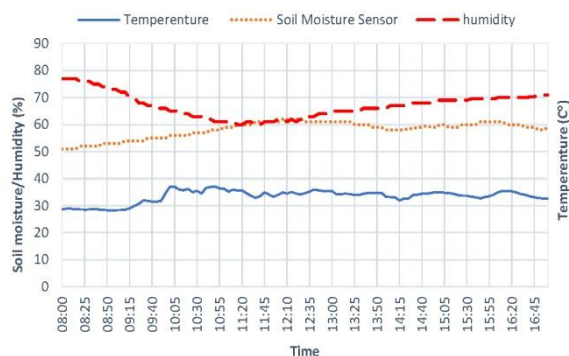


Figure 4. Monitoring of watering cassava crop systems

From figure 4 shows the experimental results of monitoring of watering cassava crop system by smartphone as follows: the average temperature of 36°C, average ambient humidity of 50%, and average soil moisture of 60%, respectively. Therefore, performance of the watering cassava crop systems with systems control using smartphone can use for the communities to reduce time, increase efficiency and increase the productivity of the community sustainably.

4. CONCLUSION

The design and development of watering cassava crop systems with systems control using smartphone. This research using solar energy for management power energy. From the experiment results of the watering cassava crop systems as follow: smartphone can ON-OFF solenoid valve to open or close water flow of 0-50 meters (diameter =100 m) in case without obstruction, 0-30 meters (diameter = 60 m) in case with obstruction, working distance of moisture sensor of 0-90 meters, water pump and solenoid valve can work precisely, respectively. Moreover, the experimental results of monitoring of watering cassava crop system by smartphone as follows: the average temperature of 36°C, average ambient humidity of 50%, and soil moisture of 60%, respectively. Therefore, the watering cassava crop systems with systems control using smartphone can use for the communities to reduce time, increase efficiency and increase the productivity of the community sustainably.

5. REFERENCES

- [1] Sun B., Jonathn Jao, Kui Wu. 2013 Wireless Sensor Based Crop Monitoring System for Agriculture Using Wi-Fi Network Dissertation. IEEE Computer Science, 280-285.
- [2] Ishak N. S., A. H. Awang, N. N. S. Bahri, and A. M. M. Zaimi 2015 GSM activated watering system prototype, IEEE International RF and Microwave Conference (RFM), 252–256.
- [3] Saha H. N., and et al. 2018 Smart Irrigation System Using Arduino and GSM Module, IEEE Annual Information Technology, Electronics and Mobile Communication Conference (IEMCON), 532–538.
- [4] Louis D., Albright, Robert W. Langhans 2015 Controlled Environment Agriculture –Scoping study, Web, September 2015.
- [5] Prema K., N. S. Kumar, S. S. Dash, and S. Chowdary 2012 Online control of remote operated agricultural robot using fuzzy controller and virtual instrumentation, IEEE-International Conference On Advances In Engineering, Science And Management (ICAESM - 2012), 196–201.
- [6] Polpitiya M. L. G., G. R. Raban, W. K. S. S. Prasanna, D. T. S. Perera, D. P. Chandima, and U. K. D. L. Udawatta 2012 Wireless agricultural sensor network, TENCON 2012 IEEE Region 10 Conference, 1–6.
- [7] dris I. and Muhammad I. S. 2012 Monitoring and control of aeroponic growing system for potato production, IEEE Conference on Control, Systems & Industrial Informatics, 120–125.
- [8] Mahamai P., Panyoyai, N., and Wacharadumrongsak, P. 2014 Automatic Watering System using Solar PV Tracking. RMUTP Research Journal. 8(2), 15-26
- [9] Thongpan N. and Thaingspak, T. 2016 Automatic Watering Systems by Wireless Sensor Network. The 2nd National Conference on Technology and Innovation Management NCTIM 2016. Rajabhat Maha Sarakham University, (30-31 March 2016), 77-84.
- [10] Kumbhar S. R. and Ghatule, A. P. 2013 Microcontroller based Controlled Irrigation System for Plantation, Proceedings of the International Multi Conference of Engineers and Computer Scientists, Hong Kong. (March 13 - 15, 2013).
- [11] Singh S., Upreti, S., Sarkar, P., and Jain, Y 2015 Arduino Based Automate Watering System, International Journal of Innovative Research in Technology, 2(6), 419-420.
- [12] Santos R., Guide for Relay Module with Arduino 2016 Random Nerd Tutorials. Available : <https://bit.ly/2BVTHYr> accessed 1st November 2018
- [13] Khemani H. 2020 What is Solenoid Valve, Bright Hub Engineering. [Online]. Available: <https://bit.ly/2Uoq60Y>, accessed 11 November 2020
- [14] The MIT Licence, 2017 Blynk. [Online]. Available: <http://docs.blynk.cc/> , accessed 11 November 2020